Journal of
Manufacturing and Materials Processing

MDPI

Article

New Self-Clinching Fasteners for Electric Conductive Connections

Rui F. V. Sampaio [1], João P. M. Pragana [1,*], Ricardo G. Clara [1], Ivo M. F. Bragança [2], Carlos M. A. Silva [1] and Paulo A. F. Martins [1]

1 IDMEC, Instituto Superior Técnico, Universidade de Lisboa, Av. Rovisco Pais, 1049-001 Lisboa, Portugal
2 CIMOSM, Instituto Superior de Engenharia de Lisboa, Instituto Politécnico de Lisboa, R. Conselheiro Emídio Navarro 1, 1959-007 Lisboa, Portugal
* Correspondence: joao.pragana@tecnico.ulisboa.pt

Abstract: This paper presents new rotational and longitudinal symmetric self-clinching fasteners to fabricate reliable connections in busbars with low electrical resistance for energy distribution systems. Connections consist of form-closed joints that are hidden inside regions where two busbars overlap. The investigation into the fabrication and performance of the new self-clinched joints involved finite element modelling and experimentation to determine the required forces and to evaluate the electric current flow and the electrical resistance at different service temperatures. The original design of the joints that was proposed in a previous work was modified to account for busbar strips of copper and/or aluminum with similar or dissimilar thicknesses, connected by means of self-clinching fasteners made from the same materials of the busbars, instead of steel. The effectiveness of the new self-clinched joints was compared to that of conventional bolted joints that are included in the paper for reference purposes. The results show that rotational symmetric self-clinching fasteners yield lighter fabrication and more compact joints with a similar electrical resistance to that of bolted joints. They also show that longitudinal symmetric self-clinching fasteners aimed at replicating the resistance-seam-welding contact conditions yield a reduction in electrical resistance to values close to that of ideal joints, consisting of two strips in perfect contact and without contaminant or oxide films along their overlapped surfaces.

Keywords: busbars; mechanical joining; self-clinching fasteners; electrical resistance; experimentation; finite element method

Citation: Sampaio, R.F.V.; Pragana, J.P.M.; Clara, R.G.; Bragança, I.M.F.; Silva, C.M.A.; Martins, P.A.F. New Self-Clinching Fasteners for Electric Conductive Connections. *J. Manuf. Mater. Process.* **2022**, *6*, 159. https://doi.org/10.3390/jmmp6060159

Academic Editor: Marion Merklein

Received: 28 November 2022
Accepted: 9 December 2022
Published: 12 December 2022

1. Introduction

Electrification is nowadays seen as one of the key strategies used to address global challenges related to environmental degradation and climate change. However, the replacement of a fossil-fuel-based economy with renewable energy sources, combined with the growing shift to electric vehicles and 5G broadband, requires an expansion of electric grids to accommodate energy demands more than ever before.

Busbars are electric grid components responsible for the transmission and distribution of energy in low-voltage, high-current applications. They are made from copper and/or aluminum strips and their use is generally preferred to the use of wires and cables because of their easiness to install and maintain, compactness, and safety [1]. In the case of electric vehicles, for example, busbars are responsible for supplying energy to electric motors, electric power steering systems and AC/DC converters, among other components.

The assembly of individual busbars into electric grids involving multiple connections is expected to cause minor disturbances in the electric current flow (i.e., to provide low electrical resistance) and to be trustworthy throughout lifetime. The fabrication of electric conductive connections (hereafter referred to as 'busbar joints') is therefore of paramount importance to the overall reliability and performance of the electric grids.

Manufacturing processes used to connect individual busbars can be classified into two main categories: (i) welding and (ii) mechanical joining [2]. Resistance spot welding and laser welding are among the most utilized welding processes, but their use is restricted by distortion and residual stresses arising from the heating–cooling cycles. They also suffer from weldability difficulties when the busbars are made from dissimilar materials (typically copper and aluminum) with different thermomechanical properties [3].

Mechanical joining comprises a much wider range of processes that can be sub-divided into two groups: (i) fastening and (ii) joining by forming [4] (Figure 1). Fastening makes use of auxiliary elements, such as bolts or conventional rivets. Bolted joints (Figure 1a) are mostly used to connect individual busbars because of their easiness in assembly and disassembly. Still, their use can be limited by bolt-head and nut protrusions above and below the busbar surfaces, and by unintentional self-loosening and non-uniform contact pressures on the overlapped busbar surfaces. The last two problems give rise to disturbances in the electric current flow that increase the electrical resistance of the joints.

Joining by forming includes all the processes in which plastic deformation is employed to produce electric conductive connections by means of form-closed and/or force-closed mechanisms. Two main subgroups are considered to yield a distinction between joining by the forming processes with no use or use of auxiliary elements [5]. Clinching (Figure 1b), for example, is a process belonging to the first subgroup (without auxiliary elements) [6] and involves the plastic deformation of both individual busbars to produce combined form-closed/force-closed electric-conductive joints [7].

Injection lap riveting [8] (Figure 1c), self-pierce riveting [9] (Figure 1d), and self-clinching [10] (Figure 1e) belong to the second subgroup (with auxiliary elements). They join by forming processes in which plastic deformation occurs mainly in the auxiliary elements, in both auxiliary elements and busbars, and mainly in the busbars, respectively. Schematic drawings illustrating the three different types of processes are enclosed in Figure 1.

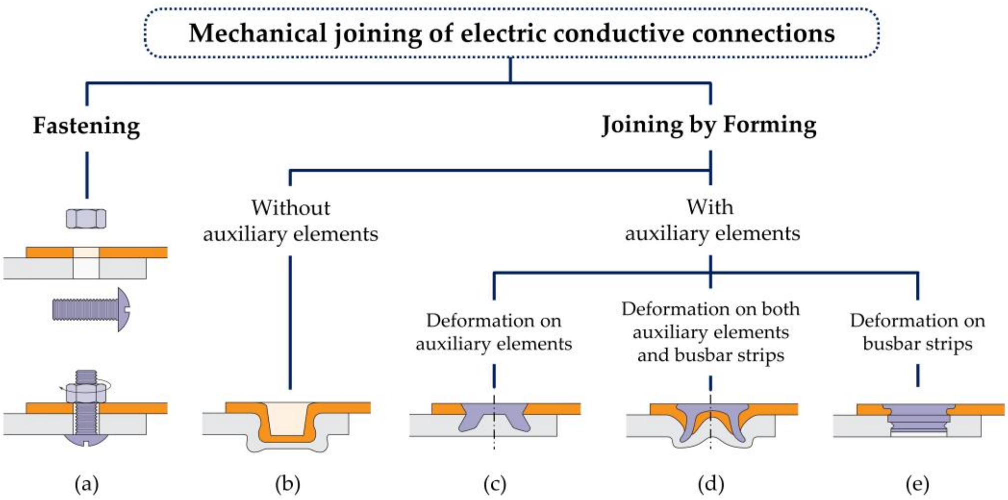

Figure 1. Types of electric conductive connections for individual busbars with schematic cross-section drawings of (**a**) bolted, (**b**) clinched, (**c**) injection lap riveted, (**d**) self-pierce riveted, and (**e**) self-clinched joints.

The process variant and joint to be addressed in this paper belong to the 'self-clinching' subgroup (Figure 1e), which needs holes with adequate dimensions to be drilled or punched into the overlapped busbars before applying a squeezing force to the fasteners (or, in some cases, to the busbars) and obtaining a form-closed/force-closed lap joint. In particular, this paper focuses on a new type of self-clinching fastener, recently developed by the authors [10], that yields the production hidden lap joints (Figure 2a).

However, unlike the previous work that was aimed at structural applications and made use of steel fasteners, the authors now focus on new design features of the joints that enhance and improve electric current flow and electrical resistance at different service temperatures [11]. The new design features consist of (i) the connection of copper and aluminum busbars with different thicknesses by means of self-clinching fasteners made from the same (or similar) materials of the busbars (Figure 2b) and (ii) the utilization of longitudinal symmetric self-clinching fasteners (Figure 2c).

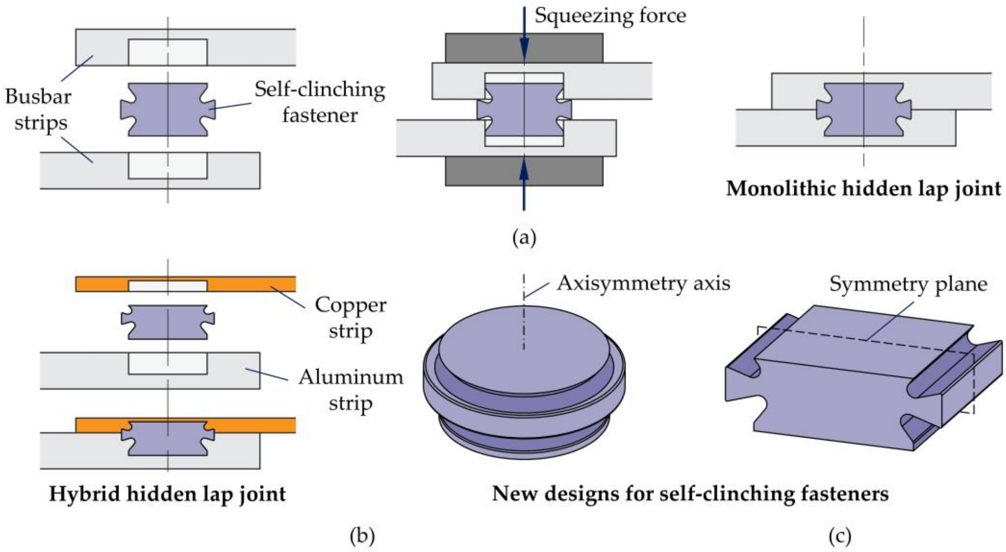

Figure 2. Self-clinching of hidden lap joints. (**a**) Schematic procedure for busbar strips made from similar materials with identical thicknesses and using steel fasteners, (**b**) new design involving different materials and thicknesses with rotational symmetric fasteners made from the same material of the individual busbar strips, (**c**) new longitudinal symmetric fastener.

The first design feature is of paramount importance for electric-conductive connections because the assembly of copper and aluminum busbars requires a combination of different thicknesses to ensure equivalent entry and exit conductance. In addition, they also require the use of copper or aluminum fasteners instead of steel to minimize disturbances in the electric current flow.

The second design feature represents a novelty in joining by forming because connections with auxiliary elements are predominantly rotation symmetric. Non-rotation symmetric joints reported in the literature, such as micro-shear clinching [12], sheet-bulk compression [13] or rectangular clinching [14], make no use of auxiliary elements; therefore, they do not belong to the group of joining by forming processes where self-clinching belongs (Figure 1). The main goal to be achieved with the second design feature is to replicate the resistance-seam-welding contact conditions, in which continuous joints are also hidden inside the regions where the two busbars overlap.

The fulfilment of the new design features yields an extension of the self-clinching hidden-lap-joint concept to electric grids. This is the main objective of this investigation, which is supported by a combination of numerical and experimental work that makes use of rotational and longitudinal symmetric self-clinching fasteners. Conventional bolted joints are used for comparison purposes.

2. Materials and Methods

The work was carried out in unit cells representing the electric-conductive connections. Both monolithic joints constructed solely from aluminum busbars and hybrid joints constructed from copper and aluminum busbars were considered to reflect the current trend in replacing copper with aluminum in all or parts of the electric grids. The research methodology involved the mechanical and thermo-electrical characterization of the busbar materials, followed by the fabrication and testing of the new joints.

2.1. Mechanical Characterization of the Materials

C11000 electrolytic copper strips (99.9% Cu) and two types of aluminum strips (AA1050-H111 with 99.5% Al and the AA6082-T6 aluminum-magnesium-silicon alloy) were utilized in multiple busbar arrangements. Self-clinching fasteners made from a high-strength AA7075-T6 aluminum alloy, with zinc as the primary alloying element, were used instead of conventional steel fasteners to minimize disturbances in the electric current flow.

The mechanical behavior of the busbar materials was characterized by means of tensile tests at the ambient temperature in specimens that were extracted from the strips and tested in accordance with ASTM standards E8/E8 M [15]. The tests were performed in an Instron 4507 universal testing machine and the resulting flow stresses, after extrapolation, are plotted in Figure 3a.

As seen from the different flow stress evolutions, the rationale behind the utilization of two different types of aluminum alloys is seen in the analysis of how dependent on the busbar material strength the self-clinched joints are.

The flow stress of the fasteners' material was determined by means of compression tests at the ambient temperature. The tests were made in cylindrical specimens of 20 mm in height and 20 mm in diameter that were machined from the AA7075-T6 aluminum rods used to produce the fasteners. The flow stress of the AA7075-T6 aluminum alloy is also included in Figure 3a.

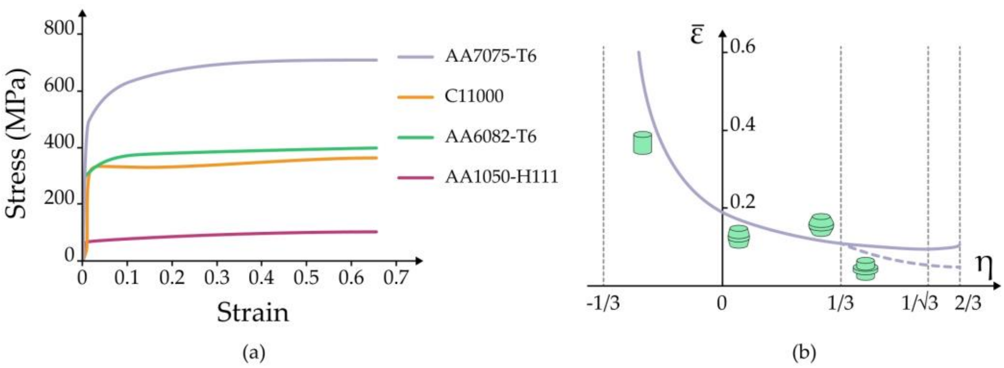

Figure 3. (**a**) Flow stress of the busbar materials and self-clinching fasteners and (**b**) fracture-forming limits of the AA7075-T6 aluminum alloy in the effective strain vs. stress triaxiality space.

The solid and dashed lines in Figure 3b represent the fracture-forming limits of the AA7075-T6 aluminum alloy in the effective strain $\bar{\varepsilon}$ vs. stress triaxiality $\eta = \sigma_m/\bar{\sigma}$ space. These lines were constructed from experimental values retrieved from conventional bulk formability tests, previously carried out by the authors [16], in cylindrical, tapered, and flanged specimens. The reason for including this information in the paper was related to the failure of self-clinching fasteners, which is addressed later in the article.

2.2. Thermo-Electrical Characterization of the Materials

The electrical resistivity of the busbar and fastener materials was determined from the electrical resistance of test specimens using a four-point probe technique [17]. The technique is based on Ohm's law and requires measurements of the voltage drop V by means of two probes spaced a distance apart (100 mm) and connected to a micro-ohmmeter KoCoS PROMET R600 that supplied an electric current of 600 A for approximately 2 s.

Figure 4 provides a scheme of the experimental setup in which an AC transformer (OFICEL 1.5 kVA) was used to pre-heat the specimens by Joule effect to a maximum temperature $T_{max} = 115$ °C (at the center). An infrared camera (FLIR E86) was employed to monitor and register the temperature. Further details on the heating, cooling, and measurement procedures are provided in [11].

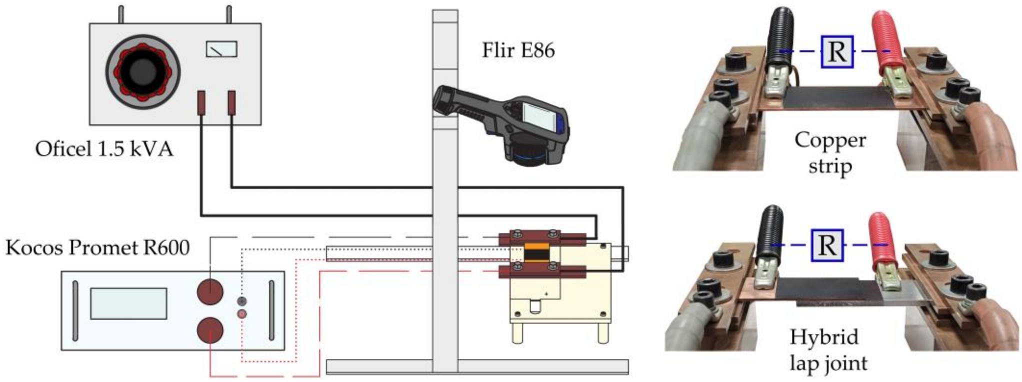

Figure 4. Schematic representation and photographs of the experimental setup utilized for the determination of the evolution of the electrical resistivity of the materials and electrical resistance of the joints with temperature.

Voltage drop measurements were taken in the cooling stage after switching off the AC transformer, within the temperature range of 105 °C to 20 °C, according to the IEEE standard for metal-clad switchgears [18]. The evolution of the electrical resistivity with temperature for the busbar and fastener materials is given in Figure 5.

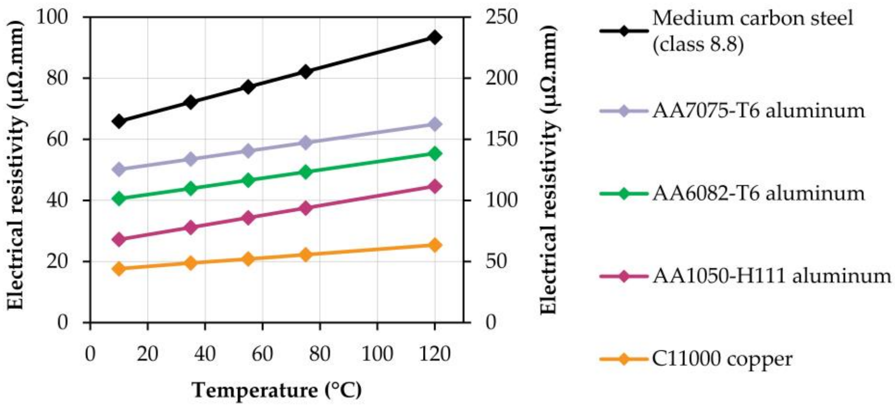

Figure 5. Evolution of the electrical resistivity with temperature for the different materials. The electrical resistivity values of the medium carbon steel must be read on the right-hand vertical axis.

The evolution of the electric resistivity with temperature for the medium carbon steel of the bolts and nuts used in conventional (reference) bolted joints was retrieved from the literature [19] and revealed much higher values than the remaining materials.

2.3. Fabrication and Testing of the Self-Clinched Joints

The experimental work on self-clinched joints made use of busbar strips with a length of 100 mm in length, width of 50 mm, and thickness of 2 mm or 5 mm. Figure 6a summarizes the fabrication route to obtain a self-clinched hybrid joint from copper and aluminum strips with $t_{Cu} = 2$ mm and $t_{Al} = 5$ mm thickness, respectively. The thickness ratio $t_{Al}/t_{Cu} = 2.5$ was close to the theoretical ratio of approximately 2.3 that ensures equal conductance in the busbars considering the electric resistivities of copper and aluminum [1] (Figure 5).

As shown, flat-bottomed (counterbore) holes or shallow pockets with different depths were first machined in adjacent regions of the busbars. Then, rotational or longitudinal symmetric self-clinching fasteners with a cross-section similar to that shown in Figure 6b were placed in position. Finally, the busbars were pressed against each other to plastically deform the material around the fasteners and create permanent form-closed hidden joints. Pressing was carried out in an Instron SATEC 1200 kN hydraulic testing machine at the ambient temperature.

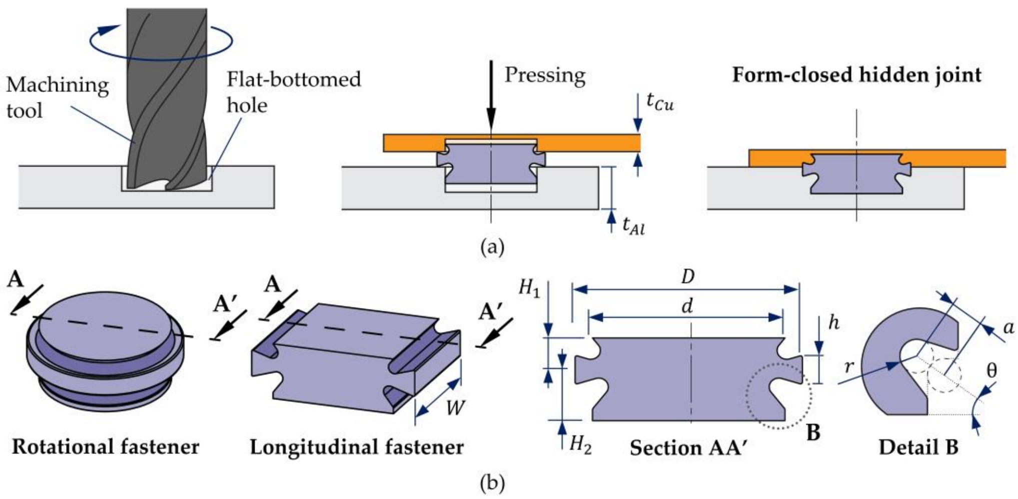

Figure 6. Self-clinched hybrid joints. (**a**) Summary of the fabrication route, (**b**) geometry and main dimensions of the rotational and longitudinal symmetric self-clinching fasteners.

The experimental and numerical development was associated with the new design features involved in the testing of monolithic and hybrid joints made from similar and dissimilar materials, with equal or different strip thicknesses, and with the use of rotational and longitudinal symmetric high-strength aluminum fasteners with an electrical resistivity similar to that of the aluminum strips. The plan of experiments is summarized in Table 1.

Table 1. The plan of experiments used in the production and analysis of busbar joints.

Monolithic Joints					
BUSBAR strip 1		Busbar strip 2		Fastener	
Material	Thickness (mm)	Material	Thickness (mm)	Material	Symmetry
AA6082-T6	5	AA6082-T6	5	AA7075-T6	Rotational
AA6082-T6	5	AA6082-T6	5	AA7075-T6	Longitudinal
Hybrid Joints					
Busbar strip 1		Busbar strip 2		Fastener	
Material	Thickness (mm)	Material	Thickness (mm)	Material	Symmetry
C11000	2	AA1050-H111	5	AA7075-T6	Rotational
C11000	5	AA1050-H111	5	AA7075-T6	Rotational
C11000	2	AA6082-T6	5	AA7075-T6	Rotational
C11000	5	AA6082-T6	5	AA7075-T6	Rotational
C11000	2	AA6082-T6	5	AA7075-T6	Longitudinal

The utilization of two types of aluminum strips with significant differences in strength compared to copper strips was intended to provide an answer to the question of how dependent the new self-clinched joints are on the material's relative strength.

The geometry of the self-clinching fasteners (refer to Figure 6b) was based on those used in a previous work of the authors [10] to obtain monolithic joints made from AA5754-H111 aluminum strips with a thickness of 5 mm and rotational symmetric AISI 316L stainless-steel fasteners. The dimensions of the rotational symmetric fasteners are given in Table 2 and include the following: (i) the outer diameter D; (ii) the semi-heights H_1 and H_2; (iii) the upper and lower head diameters d; (iv) the flange height h; (v) the fillet radius r; (vi) the depth a; and (vii) the inclination θ of the fastener annular grooves. Variations in semi-height H_1 are necessary to accommodate the connection of busbars with different thicknesses.

In the case of longitudinal symmetric fasteners, symbols D and d denote the fastener outer and head lengths, respectively, while W denotes the fastener width. The values of these dimensions were adjusted to ensure equal volume to that of the rotational symmetric fasteners for comparison purposes.

Table 2. Geometry of the self-clinching fasteners. Notation according to Figure 6b.

D (mm)	H_1 (mm)	H_2 (mm)	d (mm)	h (mm)	W (mm)	r (mm)	a (mm)	θ (°)
11.8, 13.5	1.5, 3	3	10	2.25	7.4	0.5	1.0	35

The electrical performance of the self-clinched joints with the new design features was evaluated by measuring the evolution of the electrical resistance with the temperature in the experimental setup that was previously shown in Section 2.2. Values were compared against those of conventional M8 bolted joints subjected to tightening torques of 5 Nm and 20 Nm [20].

2.4. Finite Element Analysis

Numerical simulation of the fabrication and testing of the new self-clinched joints made use of the in-house thermo-electro-mechanical finite element computer program i-form. The program was developed by the authors [21] and couples an extended version of the quasi-static flow formulation that includes elastic effects with electric potential and heat transfer equations. The weak forms of the governing mechanical (1), electrical (2), and thermal (3) equations for a continuous body with a control volume V bounded by a closed surface S, consisting of a region S_t where tractions t_i are applied and a region Sq where the heat flux q_n containing the heat dissipated by convection and radiation is defined, are given by,

$$\int_V \sigma'_{ij}\delta D_{ij} dV + \int_V K D_v \delta D_v dV - \int_{S_t} t_i \delta u_i dS = 0 \quad (1)$$

$$\int_V \nabla^2 \Phi \delta \Phi dV = 0 \quad (2)$$

$$\int_V k \nabla T \nabla(\delta T) dV - \int_{S_q} q_n \delta T dS_q + \int_V \rho c \frac{dT}{dt} \delta T dV - \int_V \beta \sigma_{ij} D_{ij} \delta T dV = 0 \quad (3)$$

The primary unknowns of each governing equation are the velocity u_i, the electric potential Φ, and the temperature T. The remaining symbols in Equations (1) to (3) are the deviatoric Cauchy stress σ'_{ij}, the rate of deformation D_{ij}, the volumetric rate of deformation D_v, the penalty function K, the thermal conductivity k, the volumetric heat capacity ρc, and the fraction β of plastic work converted into heat.

Different modelling strategies were used depending on the objectives to be attained. The fabrication of the self-clinched joints only used the mechanical engine of the finite element computer program in conjunction with axisymmetric or plane strain cross-sectional models, depending on whether rotational or longitudinal symmetric fasteners were employed. Figure 7a shows a plane strain model with approximately 5000 quadrilateral elements at the beginning and end of the joining process of a self-clinched (hidden) hybrid joint. As seen, both fastener and busbar strips were modelled as deformable objects, whereas the upper and lower squeezing (compression) platens were modelled as rigid objects and their cross-sections were discretized by means of linear contact elements.

The thermo-electric performance of the joints required the discretization of the unit cells by means of three-dimensional models built upon approximately 70,000 hexahedral elements. Symmetric conditions yielded the use of half-width size models, in which the busbars and fasteners were treated as deformable objects and the copper blocks utilized to fix the specimens and supply the electric current of 1500 A of the AC transformer during the pre-heating stage were treated as rigid objects (Figure 7b).

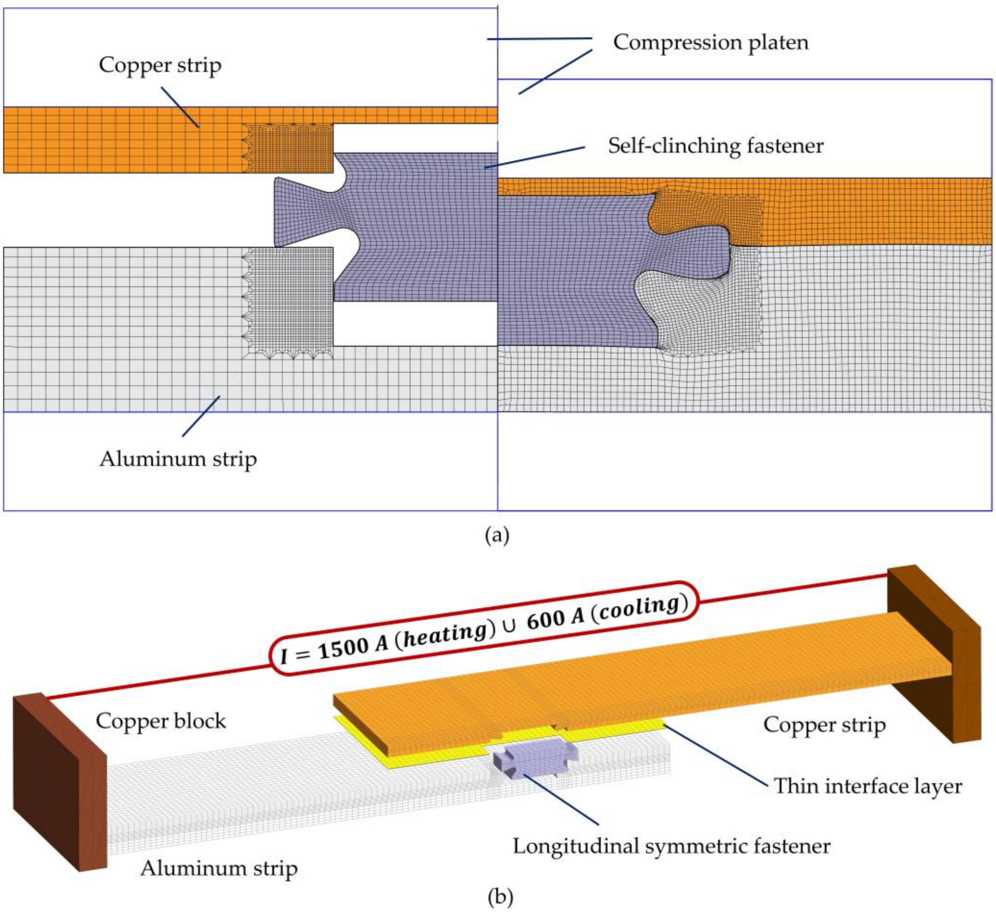

Figure 7. Finite element analysis of a self-clinched hybrid joint. (**a**) Plane strain model built upon a C11000 copper strip with a thickness of 2 mm, an AA6082-T6 aluminum strip with a thickness of 5 mm, and a longitudinal symmetric AA7075-T6 aluminum fastener, (**b**) three-dimensional model of the same joint used in the thermo-electrical analysis.

A thin interface layer with a thickness of 0.05 mm was included in the model to account for the influence of surface roughness and oxide films along the busbar overlapped region [22].

The modelling of the thermo-electrical response of the joints consisted of simulating their cooling by conduction, convection, and radiation after switching off the AC transformer and supplying an electrical current of 600 A for approximately 2 s each time the temperature dropped by approximately 10 °C, until reaching the ambient temperature (20 °C).

In the case of bolted joints, the thermo-electrical response was coupled with mechanical analysis to replicate the tightening torque put on the bolts. This was conducted through the application of an equivalent tension force at the bolts' end.

3. Results and Discussion

3.1. Rotational vs. Longitudinal Symmetric Fasteners

The first results to be presented in this section concern the comparison of self-clinched busbar joints with rotational and longitudinal symmetric fasteners in terms of their manufacturing and electrical performance. For this purpose, rotational and longitudinal symmetric fasteners with identical volumes were utilized in the fabrication of monolithic joints made from AA6082-T6 aluminum strips with a thickness of 5 mm.

Figure 8 shows the experimental and finite-element-computed cross-sections after finishing the pressing of the busbars against each other. The agreement was good and confirmed that the working principle of self-clinching remains unchanged when rotational symmetric fasteners are replaced with longitudinal symmetric fasteners. In fact, the material of the busbar strips adjacent to the longitudinal fastener was plastically deformed into the grooves of the fastener's shank, such as in the case of the rotational symmetric fastener, giving rise to a form-closed hidden joint in the region where the two busbars overlapped.

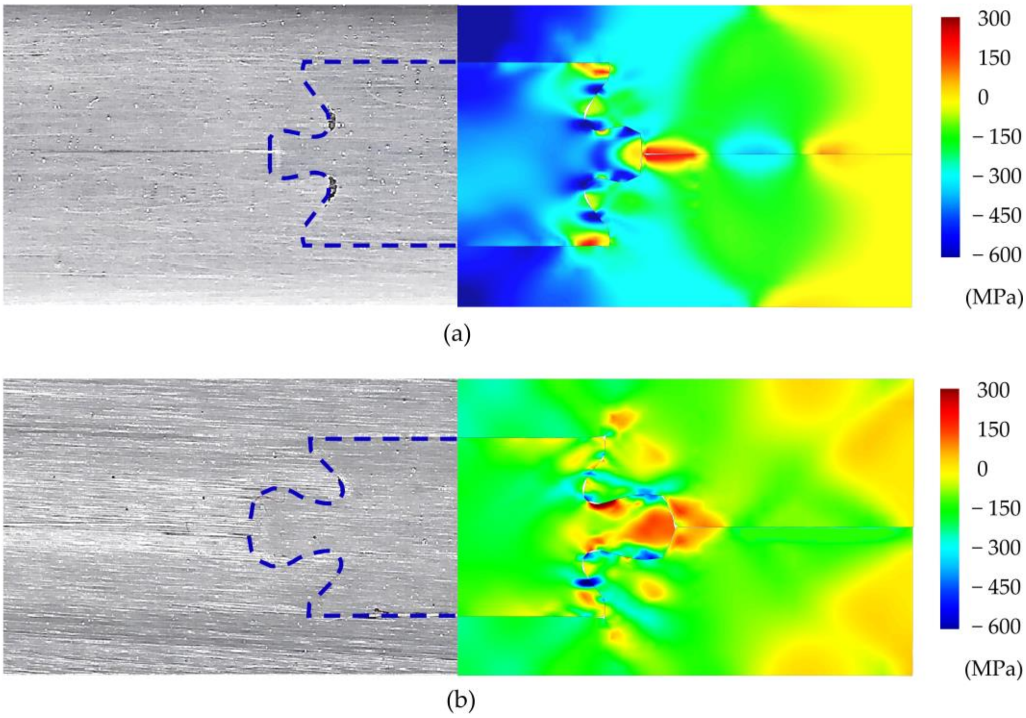

Figure 8. Experimental and finite-element-predicted cross-sections of self-clinched monolithic joints made from AA6082-T6 aluminum strips with a thickness of 5 mm using (**a**) rotational and (**b**) longitudinal symmetric AA7075-T6 aluminum fasteners. The color distributions refer to the distribution of (**a**) radial and (**b**) horizontal stresses.

However, the distributions of radial (Figure 8a) and horizontal (Figure 8b) stresses yield the conclusion that pressures along the strip-fastener-contact interfaces are considerably lower for the new longitudinal symmetric fasteners. The same applies to the evolution of the self-clinching forces with displacement that are disclosed in Figure 9. The differences in the results obtained for the two types of fasteners that are seen in Figures 8 and 9 are attributed to the replacement of the circumferential-material-flow constraint imposed by the rotational symmetric fasteners and the plane strain constraint, with lower compressive triaxiality, of the longitudinal symmetric fasteners. This explanation also helps to understand why the electrical resistance, at the ambient temperature, of the self-clinched monolithic joints with the rotational symmetric fastener (19.05 μΩ) was 3% smaller than that of the joints with longitudinal symmetric fasteners (19.60 μΩ).

However, although the electrical performance of the self-clinched joints with a single longitudinal symmetric fastener is worse than that with a single rotational symmetric fastener, this does not necessarily mean that this last type of fastener is preferable in complex joints involving longer electric conductive connection lengths, as is discussed later in the paper.

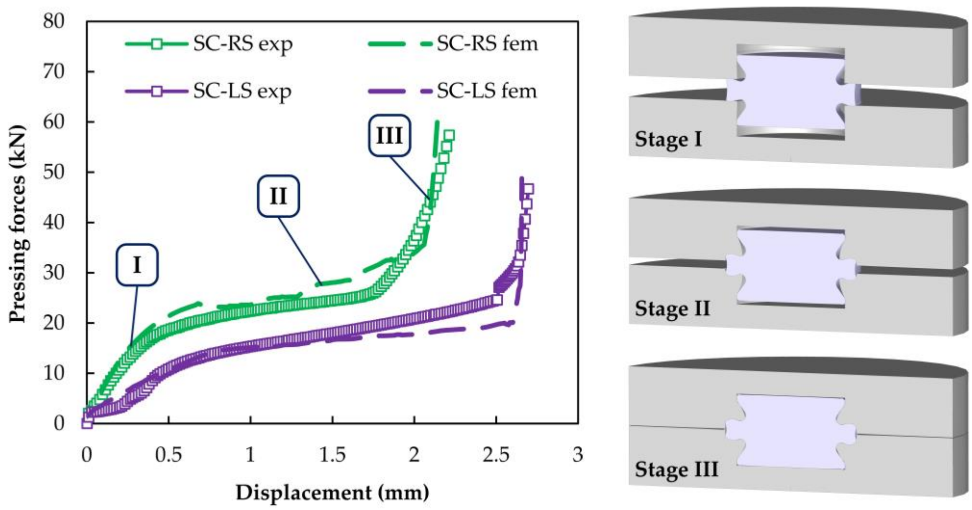

Figure 9. Experimental and finite-element-predicted evolution of the self-clinching force with displacement for monolithic joints made from AA6082-T6 aluminum strips with a thickness of 5 mm using rotational (SC-RS) and longitudinal symmetric (SC-LS) AA7075-T6 aluminum fasteners.

3.2. Hybrid Joints

The second set of results focuses on the manufacture and electric performance of self-clinched hybrid joints. For this purpose, C11000 copper strips with thicknesses of 2 mm and 5 mm were connected to AA6082-T6 aluminum strips with a thickness of 5 mm using rotational symmetric fasteners. Figure 10 shows the experimental and finite-element-computed cross-sectional joints resulting from this work, which confirms that the new self-clinching fasteners are appropriate to construct hybrid busbar joints for electric grids.

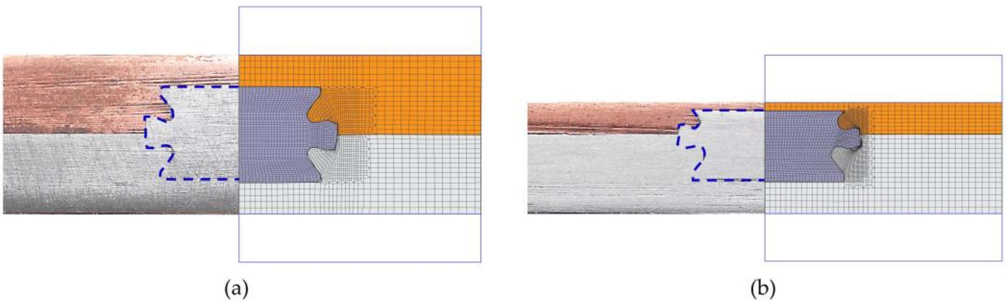

Figure 10. Experimental and finite-element-predicted cross-sections of self-clinched hybrid joints made from AA6082-T6 aluminum strips with a thickness of 5 mm and C11000 copper strips with thicknesses of (**a**) 2 mm and (**b**) 5 mm, using rotational symmetric AA7075-T6 aluminum fasteners.

The possibility of creating joints from dissimilar materials with different thicknesses, as a result of the changes made to the original design of the fasteners, deserves a special mention given its importance in ensuring equal electric conductance in the copper and aluminum busbars. The electric performance of the self-clinched hybrid joints made from C11000 copper strips with 2 mm and AA6082-T6 aluminum strips with a thickness of 5 mm was evaluated by determining the evolution of the electrical resistance with temperature in accordance with the experimental procedure that was previously described in Section 2.2. The evolution is shown in Figure 11 and consists of a straight line rising from left to right as the temperature increases, in agreement with the trend found in the electric resistivities of the different materials utilized in the joints (refer to Figure 5).

The results for the conventional bolted joints subjected to 5 and 20 Nm tightening torques are enclosed in Figure 11 for comparison purposes. They yield the conclusion that the results obtained with the self-clinched joints are analogous to those obtained with the bolted joints subjected to 20 Nm tightening torques.

The bolted joints subjected to 5 Nm provided higher values of electrical resistance and were mainly utilized to replicate relaxation due to self-loosening. This is because the normal pressures p_n acting on the overlap busbar surfaces were lower, and the electric resistivity of the thin interface layer given by $\rho^e_{int} = C/\sqrt{p_n}$ was higher, where C is a constant to be experimentally determined [22].

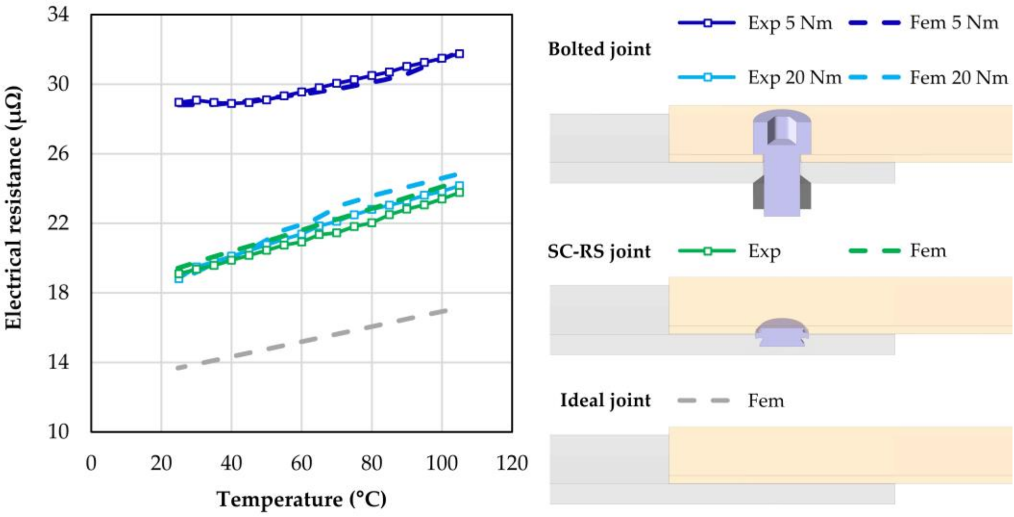

Figure 11. Experimental and finite element evolutions of the electrical resistance with temperature for the self-clinched joints with rotational symmetric (SC-RS) and longitudinal symmetric (SC-LS) fasteners and bolted hybrid joints constructed from C11000 copper strips with a thickness of 2 mm and AA6082-T6 aluminum strips with a thickness of 5 mm.

Another conclusion from the results of Figure 11 is the fact that both the self-clinched and the bolted (20 Nm) hybrid joints present electrical resistances that are substantially higher than those of an ideal hybrid joint, which consists of copper and aluminum strips in perfect contact and without a contaminant or oxide films along their overlapped surfaces (refer to the grey dashed line, obtained from finite element modelling). As is seen later in the paper, the use of multiple connections and/or longer connection lengths, yields electrical resistance values closer to those of the ideal hybrid joint.

3.3. Failure Conditions

The mechanical strength of the joints can be evaluated through destructive shear and peeling tests, among others. However, because the mechanical loads applied in electrical grids are generally low, the term failure will be used here in connection with (i) the cracking of a joint element during fabrication, or (ii) the inadmissible degradation of the electric flow capability of a joint in service.

The first case is illustrated through the unsuccessful attempt to fabricate a self-clinched hybrid joint made from C11000 copper and AA1050-H111 aluminum strips with a thickness of 5 mm using a rotational symmetric AA7075-T6 aluminum fastener. In fact, as shown in Figure 12a, the utilization of an aluminum strip much softer than the copper strip forced the latter to behave as a near rigid object and the outer flange of the fastener to bend as it penetrated the aluminum strip.

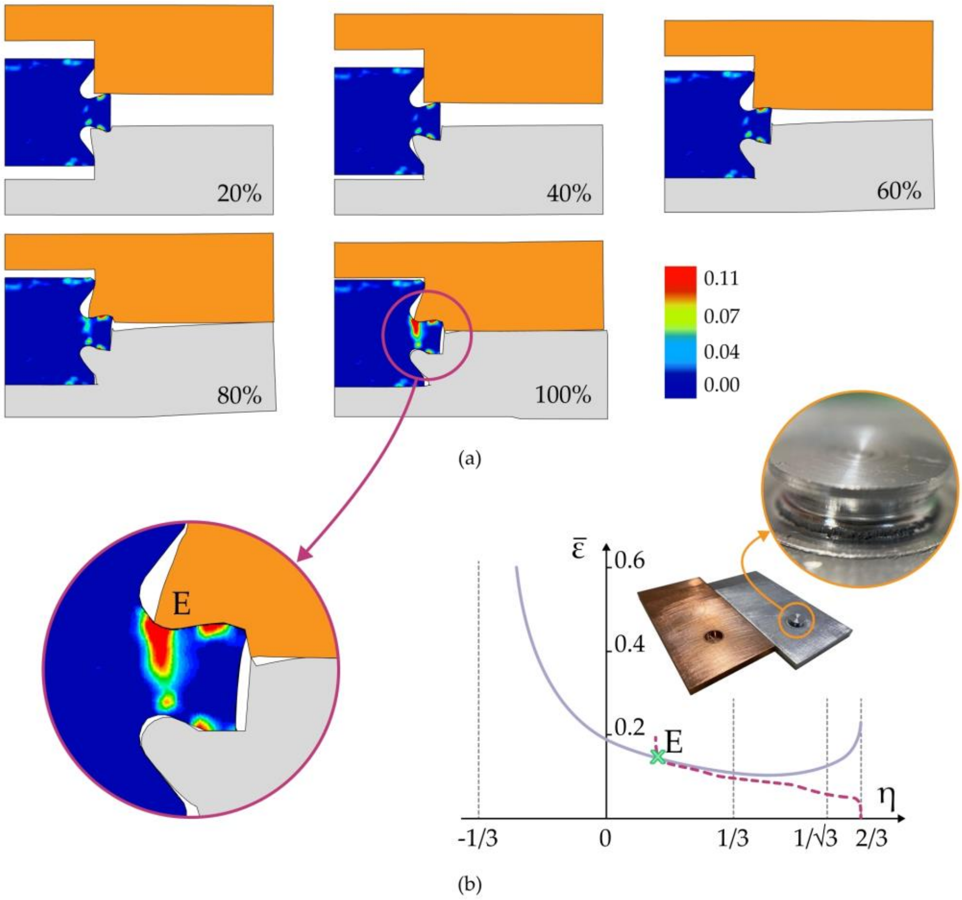

Figure 12. (**a**) Finite element computed geometry and accumulated damage during self-clinch fastening of a hybrid joint made from C11000 copper and AA1050-O aluminum strips with a thickness of 5 mm and rotational symmetric AA7075-T6 aluminum fasteners. (**b**) Loading path in the effective strain vs. stress triaxiality space for an element taken from the region E of the fastener where cracking occurred.

Ductile damage in the transition between the outer flange and the inner core of the fastener accumulated rapidly (refer to the detail in Figure 12a) and the effective strain $\bar{\varepsilon}$ in region 'E' reached values above the fracture-forming limits of the AA7075-T6 aluminum alloy that were previously introduced in Section 2.1 (Figure 12b). This led to the cracking of the self-clinching fastener, as is shown in the close-up photograph.

The accumulation of ductile damage D (Figure 12a) was calculated by means of the following ductile damage criterion for bulk metal forming built upon a combination of the Cockcroft–Latham and McClintock criteria, suitable for mode III and mode I crack opening modes, respectively [16],

$$D = \int_0^{\bar{\varepsilon}} \frac{\sigma_1}{\bar{\sigma}} d\bar{\varepsilon} + C \int_0^{\bar{\varepsilon}} \left\langle \eta - \frac{1}{3} \right\rangle^2 d\bar{\varepsilon} \quad (4)$$

where σ_1 is the major principal stress and C is a parameter determined from experiments.

Failure caused by the inadmissible degradation of the electric flow capability in service was illustrated by means of a self-clinched hybrid joint made from a C11000 copper strip with a thickness of 2 mm and AA1050-H111 aluminum strip with a thickness of 5 mm using an AA7075-T6 aluminum fastener. In fact, subjecting this joint to thermal cycles of heating and cooling raised the electrical resistance at the ambient temperature to a value of 24.37 μΩ, which is 27.5% higher than the original values of electrical resistance that were measured immediately after manufacturing. The cause for this degradation in electric performance is attributed to thermal stresses leading to the deformation of the soft AA1050-H111 aluminum strip, as well as changes in contact pressures along the interface of the fastener. Similar decreases in current-carrying capacity due to a reduction in the force–closure contact pressures have been reported in the literature for aluminum-based clinching joints [6].

3.4. Joints with Multiple or Wider Auxiliary Elements

The evolution of electrical resistance with temperature for the self-clinched hybrid joints that was previously discussed in Section 3.2 raises the question of how to improve electric performance to reach values close to that of an ideal hybrid joint.

The most common strategy in the case of bolted hybrid joints consists of increasing the number of bolts per overlapped surface (Figure 13a) to extend the region subjected to high contact pressure [23,24]. This helps flatten the asperities and break the films across the contact interfaces.

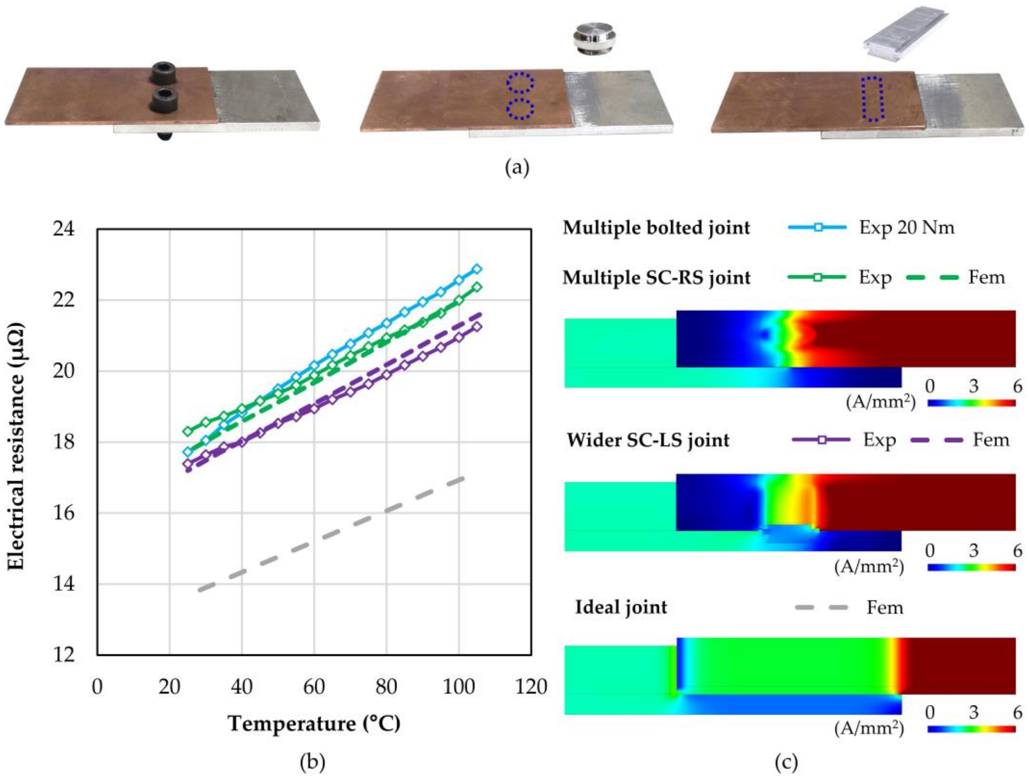

Figure 13. (**a**) Hybrid joints made from C11000 copper strips with a thickness of 2 mm and AA6082-T6 aluminum strips with a thickness of 5 mm and multiple (left and middle) and wider (right) auxiliary elements, (**b**) experimental evolution of electrical resistance with temperature for the different joints shown in (**a**), and (**c**) finite element distribution of current density (A/mm^2) for the ideal and self-clinched hybrid joints with two rotational symmetric fasteners and one, wider, longitudinal symmetric fastener.

Figure 13b shows the evolution of the electrical resistance with temperature, from which it can be seen that joints with two bolts provided results closer to those of the ideal hybrid joint. However, this decrease in electrical resistance came at the price of increasing the weight of the joints by approximately 9.5% compared that of single-bolted joints.

The use of self-clinched joints with two rotational symmetric fasteners (Figure 13a) provided gains in performance with respect to self-clinched joints with one rotational symmetric fastener that are compatible with those previously observed in bolted joints. The advantage of bolted joints is that the gain in performance is achieved without increasing the weight of the joints.

Further improvements in the electrical performance of the self-clinched joints can, however, be achieved by means of longitudinal symmetric fasteners (Figure 13a) due to the formation of a hidden connection aimed at replicating the continuous contact conditions of resistance seam welding. The evolution of electrical resistance with temperature is enclosed in Figure 13b, and the reason for providing values closer to the ideal hybrid joint was attributed to a significant reduction in electric current disturbances at the center of the overlapped busbar surfaces (Figure 13c).

The focus on thermo-electrical instead of mechanical performance, as is common in mainstream research on joining by plastic deformation, is because mechanical loading applied in electric grids is generally low. Still, future research directions in the field may account for the mechanical performance of the joints by means of quasi-static destructive tests whenever short-circuit events in electric grids are to be considered.

4. Conclusions

Self-clinching fasteners with various design features can be successfully utilized to fabricate reliable busbar hybrid joints with low electrical resistance, made from dissimilar materials (e.g., copper and aluminum) with different strip thicknesses, for energy distribution systems.

Self-clinched joints are lighter and more compact than conventional bolted joints and provide values of electrical resistance that are 11% smaller (in average) due to the replacement of the steel bolts and nuts by aluminum fasteners with much smaller electric resistivity. The electrical resistance of the self-clinched hybrid joints increased by approximately 26% when the service temperature was raised from 20 °C to 105 °C.

Differences in strength between busbar materials must be kept small. This is necessary to prevent near-rigid object behaviors and the cracking of the fasteners during self-clinching, as well as the degradation of the electrical performance of the joints during heating–cooling service cycles.

Wider longitudinal symmetric fasteners are a good alternative to bolted and self-clinched joints with multiple bolts or rotational symmetric fasteners due to their ability to provide continuous lap joints with better electrical performance and no increase in weight.

Author Contributions: Conceptualization, I.M.F.B., C.M.A.S. and P.A.F.M.; methodology, I.M.F.B., C.M.A.S. and P.A.F.M.; software, R.F.V.S., R.G.C., J.P.M.P. and P.A.F.M.; validation, R.G.C. and J.P.M.P.; formal analysis, R.F.V.S., R.G.C., J.P.M.P., I.M.F.B., C.M.A.S. and P.A.F.M.; investigation, R.F.V.S., R.G.C., J.P.M.P., I.M.F.B., C.M.A.S. and P.A.F.M.; resources, I.M.F.B., C.M.A.S. and P.A.F.M.; writing—original draft preparation, R.G.C., J.P.M.P. and P.A.F.M.; writing—review and editing, R.G.C., J.P.M.P., I.M.F.B., C.M.A.S. and P.A.F.M.; visualization, R.G.C. and J.P.M.P.; supervision, I.M.F.B., C.M.A.S. and P.A.F.M.; project administration, P.A.F.M.; funding acquisition, P.A.F.M. All authors have read and agreed to the published version of the manuscript.

Funding: This research was funded by Fundação para a Ciência e a Tecnologia of Portugal and IDMEC under LAETA-UIDB/50022/2020 and PTDC/EME-EME/0949/2020.

Institutional Review Board Statement: Not applicable.

Informed Consent Statement: Not applicable.

Data Availability Statement: All data supporting the reported results are available in the paper.

Acknowledgments: The authors would like to thank the support provided by Fundação para a Ciência e a Tecnologia of Portugal and IDMEC under LAETA-UIDB/50022/2020 and PTDC/EME-EME/0949/2020.

Conflicts of Interest: The authors declare no conflict of interest.

References

1. Sampaio, R.F.V.; Zwicker, M.F.R.; Pragana, J.P.M.; Bragança, I.M.F.; Silva, C.M.A.; Nielsen, C.V.; Martins, P.A.F. Busbars for e-mobility: State-of-the-art review and a new joining by forming technology. In *Mechanical and Industrial Engineering: Historical Aspects and Future Directions*; Davim, J.P., Ed.; Springer: Berlin, Germany, 2022; pp. 111–141.
2. Bao, Y.J.; Cheng, K.W.E.; Ding, K.; Wang, D.H. The study on the busbar system and its fault analysis. In Proceedings of the 5th International Conference on Power Electronics Systems and Applications (PESA), Hong Kong, China, 11–13 December 2013; pp. 1–7.
3. Sudhanshu, T.; Panda, S. Characterisation of Cu–Al alloy lap joint using tig welding. *CIRP J. Manuf. Sci. Technol.* **2021**, *35*, 454–459.
4. Salamati, M.; Soltanpour, M.; Fazli, A.; Zajkani, A. Processing and tooling considerations in joining by forming technologies; Part A–Mechanical joining. *Int. J. Adv. Manuf. Technol.* **2019**, *101*, 261–315. [CrossRef]
5. Meschut, G.; Merklein, M.; Brosius, A.; Drummer, D.; Fratini, L.; Füssel, U.; Gude, M.; Homberg, W.; Martins, P.A.F.; Bobbert, M.; et al. Review on mechanical joining by plastic deformation. *J. Adv. Join. Process.* **2022**, *5*, 100113. [CrossRef]
6. Kalich, J.; Füssel, U. Influence of the production process on the binding mechanism of clinched aluminum steel mixed compounds. *J. Manuf. Mater. Process.* **2021**, *5*, 105. [CrossRef]
7. Füssel, U.; Schlegel, S.; Reschke, G.; Kalich, J. Electrical contacting of aluminum bus bars using clinching and functional elements. *Eng. Proc.* **2022**, *26*, 5. [CrossRef]
8. Ferreira, F.R.; Pragana, J.P.M.; Bragança, I.M.F.; Silva, C.M.A.; Martins, P.A.F. Injection lap riveting. *CIRP Ann. Manuf. Technol.* **2021**, *70*, 261–264. [CrossRef]
9. Abe, Y.; Maeda, T.; Yoshioka, D.; Mori, K.-I. Mechanical clinching and self-pierce riveting of thin three sheets of 5000 series aluminium alloy and 980 mpa grade cold rolled ultra-high strength steel. *Materials* **2020**, *13*, 4741. [CrossRef] [PubMed]
10. Sampaio, R.F.V.; Pragana, J.P.M.; Bragança, I.M.F.; Silva, C.M.A.; Martins, P.A.F. A self-clinching fastener for hidden lap joints. *CIRP J. Manuf. Sci. Technol.* **2022**, *37*, 434–442. [CrossRef]
11. Pragana, J.P.M.; Sampaio, R.F.V.; Bragança, I.M.F.; Silva, C.M.A.; Martins, P.A.F. Injection lap riveting of aluminum busbars—A thermo-electro-mechanical investigation. *J. Manuf. Mater. Process.* **2022**, *6*, 74. [CrossRef]
12. Li, X.; Wang, X.; Shen, Z.; Ma, Y.; Liu, H. An experimental study on micro-shear clinching of metal foils by laser shock. *Materials* **2019**, *12*, 1422. [CrossRef] [PubMed]
13. Reichel, A.; Sampaio, R.F.; Pragana, J.P.M.; Bragança, I.M.F.; Silva, C.M.A.; Martins, P.A.F. Form-fit joining of hybrid busbars using a flexible tool demonstrator. *Proc. Inst. Mech. Eng. Part L J. Mater. Des. Appl.* **2022**, *236*, 1164–1175. [CrossRef]
14. Lambiase, F.; Scipioni, S.I.; Lee, C.-J.; Ko, D.-C.; Liu, F.A. State-of-the-art review on advanced joining processes for metal-composite and metal-polymer hybrid structures. *Materials* **2021**, *14*, 1890. [CrossRef] [PubMed]
15. *ASTM E8/E8M*; Standard Test Methods for Tension Testing of Metallic Materials. ASTM: West Conshohocken, PA, USA, 2010; pp. 1–27.
16. Sampaio, R.F.V.; Pragana, J.P.M.; Bragança, I.M.F.; Silva, C.M.A.; Martins, P.A.F. Revisiting the fracture forming limits of bulk forming under biaxial tension. *Int. J. Damage Mech.* **2022**, *31*, 882–900. [CrossRef]
17. Kumar, N.; Masters, I.; Das, A. In-depth evaluation of laser-welded similar and dissimilar material tab-to-busbar electrical interconnects for electric vehicle battery pack. *J. Manuf. Process.* **2021**, *70*, 78–96. [CrossRef]
18. *IEEE Std C37.20.2*; IEEE Standard for Metal-Clad Switchgear. IEEE Power and Energy Society: New York, NY, USA, 2015.
19. MatWeb. Available online: https://www.matweb.com (accessed on 1 October 2022).
20. Sampaio, R.F.V.; Pragana, J.P.M.; Bragança, I.M.F.; Silva, C.M.A.; Nielsen, C.V.; Martins, P.A.F. Electric performance of fastened hybrid busbars: An experimental and numerical study. *J. Mater. Des. Appl.* **2022**, *263*, 1152–1163. [CrossRef]
21. Nielsen, C.V.; Martins, P.A.F. *Finite element flow formulation In Metal Forming: Formability, Simulation and Tool Design*; Academic Press: London, UK, 2021; pp. 181–249.
22. Studer, F.J. Contact resistance in spot welding. *Weld. J.* **1939**, *18*, 374–380.
23. Tzeneva, R.; Slavtchev, Y.; Mladenov, V. New connection design of high-power bolted busbar connections. In Proceedings of the 11th WSEAS International Conference on Circuits, Agios Nikolaos, Greece, 23–25 July 2007; pp. 228–233.
24. Moustafa, G.; Grossmann, S.; Abdel-Salam, M.; Dessouky, S.S.; El-Makkawy, S.M. Joint resistance of bolted copper bus-bar connections as influenced by mechanical contact devices material and configuration. In Proceedings of the 13th Middle East Power Systems Conference (MEPCON), Assiut, Egypt, 20–23 December 2009; pp. 300–305.